

## Threshold behavior of (GaAl)As-GaAs lasers at low temperatures

C. J. Hwang, N. B. Patel, M. A. Sacilotti, F. C. Prince, and D. J. Bull

Citation: *Journal of Applied Physics* **49**, 29 (1978); doi: 10.1063/1.324384

View online: <http://dx.doi.org/10.1063/1.324384>

View Table of Contents: <http://scitation.aip.org/content/aip/journal/jap/49/1?ver=pdfcov>

Published by the [AIP Publishing](http://www.aip.org)

---

### Articles you may be interested in

[Near-ideal low threshold behavior in \(111\) oriented GaAs/AlGaAs quantum well lasers](#)

*Appl. Phys. Lett.* **52**, 339 (1988); 10.1063/1.99457

[Low threshold operation of a GaAlAs/GaAs distributed feedback laser with double channel planar buried heterostructure](#)

*Appl. Phys. Lett.* **49**, 1145 (1986); 10.1063/1.97448

[Room-temperature pulsed oscillation of GaAlAs/GaAs surface emitting injection laser](#)

*Appl. Phys. Lett.* **45**, 348 (1984); 10.1063/1.95265

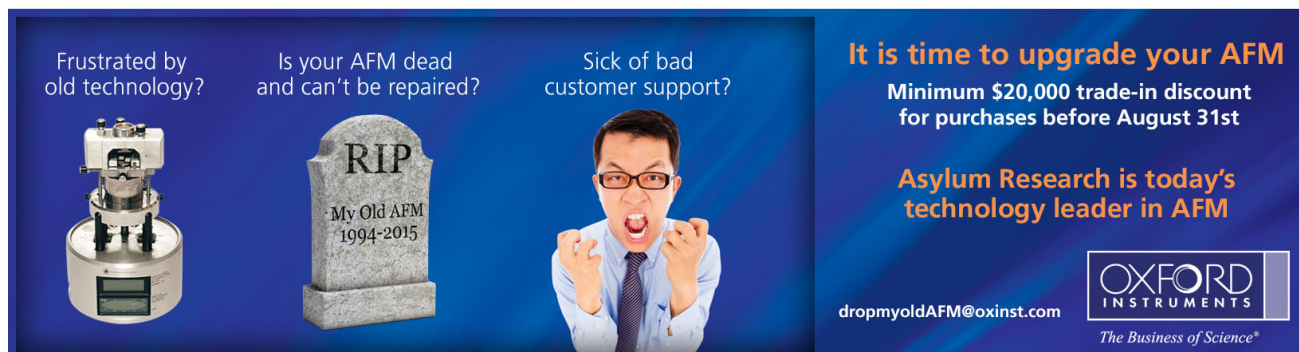
[Very low threshold-current temperature sensitivity in constricted double-heterojunction AlGaAs lasers](#)

*J. Appl. Phys.* **52**, 3840 (1981); 10.1063/1.329846

[Narrow-beam five-layer \(GaAl\)As/GaAs heterostructure lasers with low threshold and high peak power](#)

*J. Appl. Phys.* **47**, 1501 (1976); 10.1063/1.322816

---

An advertisement for Oxford Instruments' AFM technology. The background is dark blue. On the left, there is an image of a white AFM instrument. In the center, there is a grey tombstone with the inscription 'RIP My Old AFM 1994-2015'. To the right of the tombstone is a man in a white shirt and tie, looking frustrated with his hands clenched in fists. Text on the left asks 'Frustrated by old technology?', 'Is your AFM dead and can't be repaired?', and 'Sick of bad customer support?'. On the right, it says 'It is time to upgrade your AFM', 'Minimum \$20,000 trade-in discount for purchases before August 31st', and 'Asylum Research is today's technology leader in AFM'. At the bottom right, there is the Oxford Instruments logo and the tagline 'The Business of Science®'. An email address 'dropmyoldAFM@oxinst.com' is also provided.

# Threshold behavior of (GaAl)As-GaAs lasers at low temperatures

C. J. Hwang<sup>a)</sup>

*Hewlett-Packard Laboratories, 1501 Page Mill Road, Palo Alto, California 94304*

N. B. Patel, M. A. Sacilotti, F. C. Prince, and D. J. Bull

*Instituto de Fisica, Universidade Estadual de Campinas, 13.100, Campinas, S.P. Brazil*

(Received 6 July 1977; accepted for publication 25 August 1977)

The temperature dependence of the threshold current, differential quantum efficiency, and internal loss have been measured in the temperature range 10–293°K. The threshold current increases relatively slowly with temperature above 100°K and is independent of the impurity concentration. Theoretical calculation shows that this behavior is to be expected for a band-to-band transition that follows  $k$  selection. The threshold behavior at low temperatures ( $\leq 80^\circ\text{K}$ ) depends strongly on the type and concentration of the impurity. The relatively fast decrease in threshold below 100°K shows saturation for an active layer with  $n$ -type impurities or with high-concentration  $p$ -type impurities. The saturation is attributed to the carrier diffusion length becoming smaller than the active-layer thickness. The internal differential quantum efficiency is near unity and is independent of temperature. The internal loss, however, decreases with temperature due to reduction in free-carrier absorption.

PACS numbers: 42.55.Px, 85.60.Jb, 78.45.+h

## I. INTRODUCTION

During the early stage of laser development, temperature dependence of threshold current below room temperature was important because it gave information about the highest temperature that a homostructure laser would operate continuously.<sup>1–5</sup> From these studies, phenomena such as long time delay,<sup>6</sup> internal Q switching,<sup>6</sup> and bistable operation<sup>7,8</sup> of lasers were discovered. Furthermore, the experimental temperature dependence of threshold current was used to test the various theories on semiconductor lasers.<sup>9–14</sup> With the invention of double-heterostructure (DH) lasers, cw operation at room temperature or higher is no longer a problem, and there is less interest in low-temperature behavior. Some work has been reported for temperature dependence of threshold down to 80°K<sup>15,16</sup> for early DH lasers with broad contacts having relatively high threshold current density. This paper represents the first attempt to study state-of-the-art stripe-geometry DH lasers at temperatures down to 10°K. We measure the light output as a function of current for lasers with different cavity lengths to obtain not only the temperature dependence of threshold current and external differential quantum efficiency but also to derive the temperature dependence of internal optical loss and internal differential quantum efficiency. The threshold behavior at low temperatures ( $\leq 40^\circ\text{K}$ ) depends strongly on the impurity density in the active region of which the high-temperature ( $\geq 80^\circ\text{K}$ ) behavior is relatively independent. It is concluded that the transition is of the band-to-band type which obeys the  $k$  selection at least down to 80°K. The low-temperature behavior is determined by the relative value of the carrier diffusion length with respect to the thickness of the active region. If the diffusion length is smaller than the width of the active region, the threshold current saturates;

otherwise, the threshold current decreases monotonically to 2 or 3 mA at 10°K. In Sec. II, we describe the general properties of our lasers and the experimental arrangement for the measurements. In Sec. III, we present and discuss our results.

## II. EXPERIMENTAL

The lasers used are stripe-geometry four-layer DH devices similar to the ones described elsewhere.<sup>17</sup> The stripe contact, 13  $\mu\text{m}$  wide, is formed by proton bombardment<sup>18</sup> which does not reach the active region. The active layer thickness is 0.2  $\mu\text{m}$ . The length of the laser varies from 180 to 610  $\mu\text{m}$ . Our standard laser is 380  $\mu\text{m}$  long and has typical threshold current and differential quantum efficiency of 80 mA and 40%, respectively, at room temperature. Hall measurements were made on a single layer grown on a semi-insulating substrate to determine the active-layer carrier concentration at various dopings. The acceptor concentration was then obtained according to the analysis described in Ref. 19. In the case of a compensated active layer, the donor or the acceptor concentration was assumed to be the same as that in the respective noncompensated  $n$ - or  $p$ -type layer grown with the same amount of donor or acceptor dopant in the Ga solution.

Since the meaningfulness of the present experiment depends critically on the extent of the data scatter, we selected wafers which yield lasers with a variation of threshold and differential quantum efficiency of no more than 10% for randomly chosen 10 lasers at a fixed cavity length. Furthermore, we required that the lasers have linear output up to  $\sim 9$  mW from one cavity face for a wide range of temperatures and that the output characteristics from both faces be identical. The threshold current is taken as the intersection between the extrapolated spontaneous-emission curve below the threshold and stimulated-emission curve above the threshold. The differential quantum efficiency is determined from the slope of the stimulated emission curve.

<sup>a)</sup>Present address: General Optronics, Corp., 3005 Hadley Road, South Plainfield, N.J. 07080.

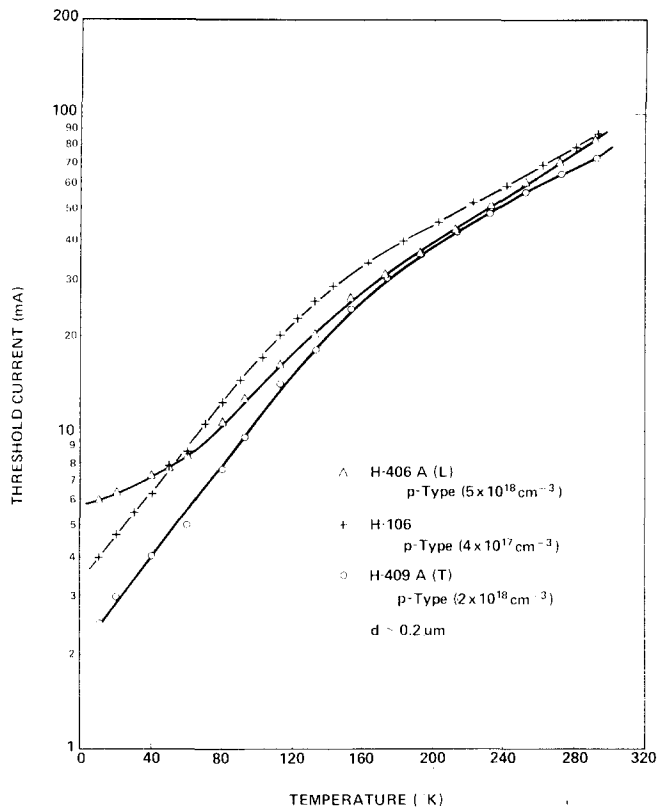


FIG. 1. Temperature dependence of threshold current for DH lasers with three different doping concentrations in the active layers.

The diode was placed in an evacuated He exchange Dewar whose temperature could be varied from 10 to 297 °K. The laser was driven with a 200-ns pulse at 1 kHz. A current probe was used to monitor the current directly. This direct current measurement is essential since the resistance of the laser changes substantially with temperature and the usual technique of converting the voltage across the laser and a series resistor to the current is not practical.

### III. RESULTS AND DISCUSSION

#### A. Temperature behavior of threshold current

Figure 1 shows the temperature dependence of threshold current for standard lasers with active-layer impurity concentrations of  $4 \times 10^{17}$  (H106),  $2 \times 10^{18}$  (H409), and  $5 \times 10^{18}$  (H406). These lasers all have about the same active-layer thickness of  $\sim 0.2 \mu\text{m}$ . The behavior above 80 °K for the three types of lasers is very similar, namely, the threshold increases at about the same rate with temperature and the absolute value of the threshold current is about the same. The situation is, however, quite different at low temperatures. For the low-doped case ( $\leq 2 \times 10^{18} \text{ cm}^{-3}$ ), the threshold current keeps decreasing to the lowest temperature used (10 °K). The threshold current at this temperature is low, i. e., 2–3 mA (40–60 A/cm<sup>2</sup>). We believe that this is the first time such a low value of threshold current has been reported. For the more heavily doped case ( $\geq 5 \times 10^{18} \text{ cm}^{-3}$ ), the threshold current shows saturation at low temperatures ( $\leq 80 \text{ °K}$ ). We find that the lower the

doping, the lower the saturation temperature. Thus, it is possible that the saturation may occur below 10 °K for the low-doped case ( $\approx 2 \times 10^{18} \text{ cm}^{-3}$ ). Figure 2 shows the temperature dependence of threshold current for a compensated active region (H407,  $N_A = 5 \times 10^{18} \text{ cm}^{-3}$  and  $N_D = 4 \times 10^{16} \text{ cm}^{-3}$ ) and an *n*-type active region (H235,  $N_D = 4 \times 10^{16} \text{ cm}^{-3}$ ). The threshold behavior for both cases is again similar to that shown in Fig. 1 in the high-temperature region. However, the saturation occurs at higher temperatures (100 °K) for the compensated case than the one without compensation. Also, it occurs for the *n*-type active region even though the doping is relatively low.

The fact that the threshold behavior is independent of doping at high temperatures for a wide range of *p*-type impurity concentration indicates that the carrier recombination is not modified by the presence of the impurities. This can only happen when the transition is from the conduction band to the valence band. The saturation at low temperature for active regions of *n* type and for highly doped *p* type with and without compensation is similar to that observed in homostructure<sup>1–3</sup> and single-heterostructure lasers.<sup>4</sup> This indicates the existence of incomplete carrier and optical confinement. The same situation can occur in DH lasers if the carrier diffusion length is smaller than the active-layer thickness.

The value of carrier diffusion length depends on the carrier lifetime and the diffusion constant. At temperatures below 100 °K, the total cavity loss is less than 50 cm<sup>-1</sup> [internal loss  $\leq 20 \text{ cm}^{-1}$  (Sec. III B) and mirror loss = 30 cm<sup>-1</sup> for the standard length of 380  $\mu\text{m}$ ]. The

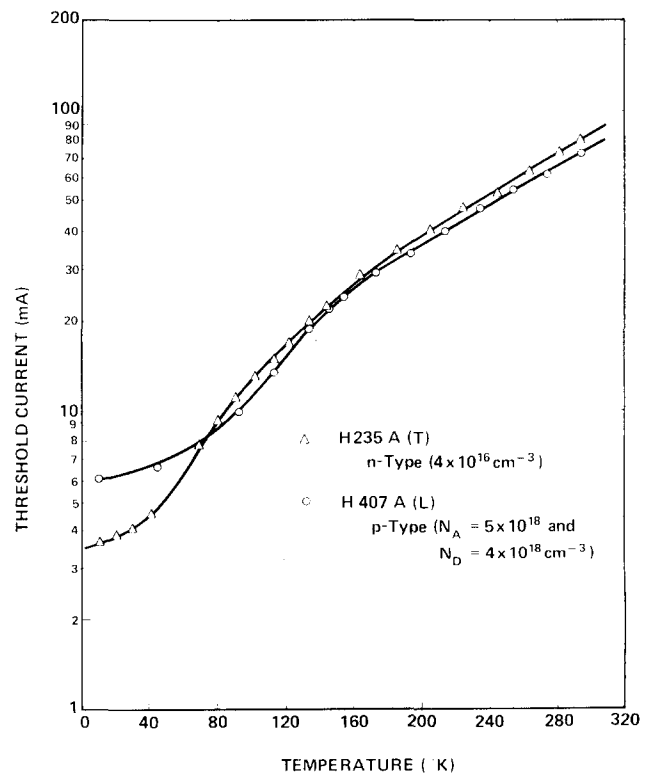


FIG. 2. Temperature dependence of threshold current for DH lasers with a compensated and an *n*-type active layer.

injected carrier density required to reach the threshold below 100 °K is  $\leq 3 \times 10^{17} \text{ cm}^{-3}$  according to the calculation of Stern,<sup>14</sup> which will be further discussed later in this paper. Since our lowest  $p$  doping in the active layer is  $4 \times 10^{17} \text{ cm}^{-3}$ , the minority-carrier (electron) diffusion length determines the recombination region in the case of  $p$ -type active regions with the without compensation. In the case of low-doped  $n$ -type active regions, the hole diffusion length determines the recombination region.

In a medium in which the carrier recombination efficiency is close to unity, the carrier lifetime is nearly equal to the radiative lifetime which is roughly inversely proportional to the majority-carrier concentration. Thus, qualitatively, the higher the impurity concentration, the shorter the minority-carrier lifetime. The carrier diffusion constant can be expressed as  $\mu E_d / e$ ,<sup>19-21</sup> where  $\mu$  is the mobility,  $E_d$  is the diffusion energy, and  $e$  is the electron charge. As a first approximation,  $E_d \approx kT$ <sup>19-21</sup> and therefore decreases with temperature. The mobility at low temperatures is mainly determined by the impurity scattering.<sup>22</sup> The mobility should be lower with higher impurity concentration. It should be lowest in the highly compensated case because of the reduction in the carrier screening effect.<sup>23,24</sup> Furthermore, holes should have a lower mobility than electrons. Thus, we can qualitatively state the following: It is possible that the carrier diffusion length is shorter for a more heavily doped  $p$  active layer and shortest for a compensated active region. The holes have a shorter diffusion length than the electrons for the same impurity concentration.

We conclude that the temperature at which the diffusion length is equal to the active-layer thickness (the saturation temperature) is higher for a more heavily doped case and highest for the compensated case. It is also higher for  $n$ -type active layers than for the  $p$ -type active layer with the same doping. This conclusion is of course consistent with our experimental observations shown in Figs. 1 and 2.

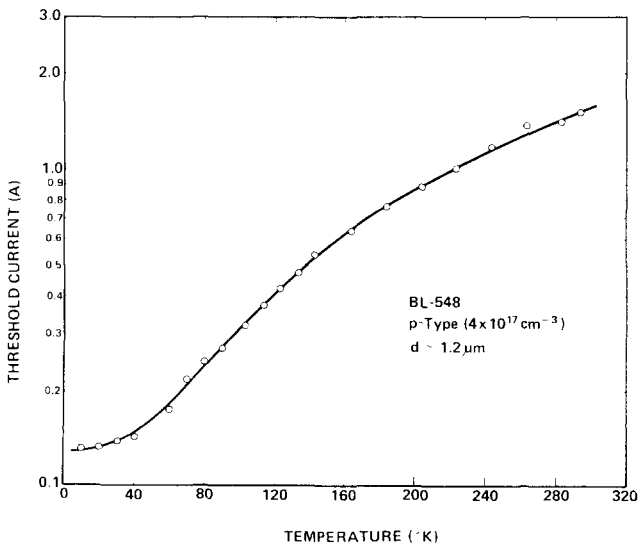


FIG. 3. Temperature dependence of threshold current for a DH laser with a thick active layer.

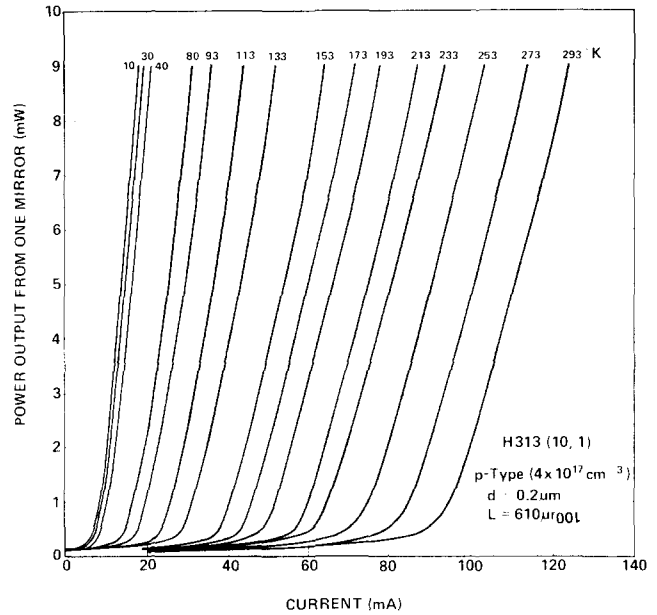


FIG. 4. Light output as a function of current input at various temperatures.

As an additional substantiation of the diffusion-length model, we show in Fig. 3 a laser with larger active-layer thickness ( $1.2 \mu\text{m}$ ) but with the same  $p$ -doping ( $4 \times 10^{17} \text{ cm}^{-3}$ ) as laser H106 shown in Fig. 1. Other parameters are identical. The high-temperature behavior is again similar to those shown in Figs. 1 and 2. However, the laser with wider active regions shows saturation at  $\sim 50^\circ\text{K}$ .

### B. Temperature behavior of internal loss

As was pointed out in Sec. III A, the behavior of threshold current above  $80^\circ\text{K}$  does not depend on the impurity concentration and hence indicates a band-to-band recombination. In order to show that the transition is indeed band to band quantitatively, we calculate the temperature dependence of threshold current using a

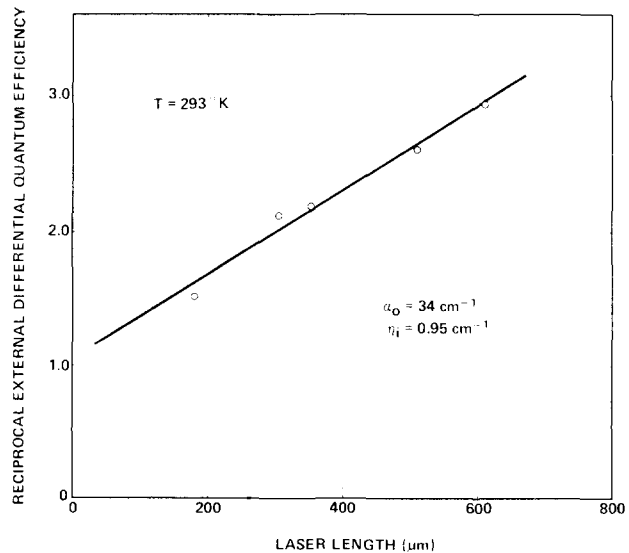


FIG. 5. Variation of the reciprocal external differential quantum efficiency with the laser cavity length.

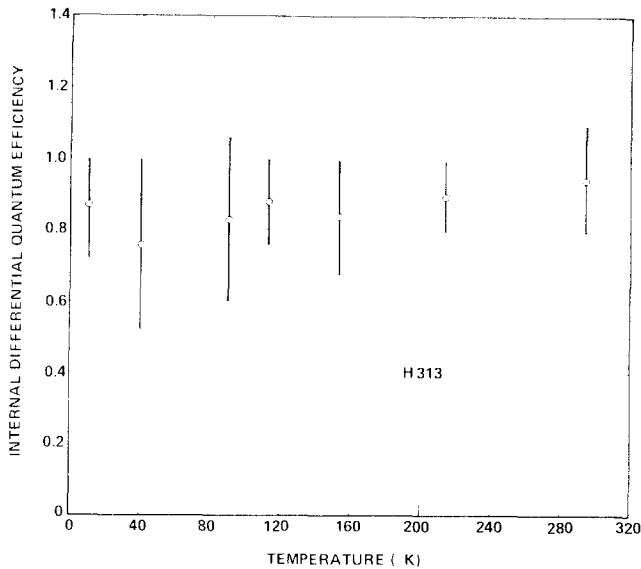


FIG. 6. Variation of the internal differential quantum efficiency with temperature.

band-to-band recombination theory derived by Stern.<sup>14</sup> To do this, however, we need to know the temperature dependence of the internal loss. Consequently, the external differential quantum efficiency  $\eta$  was measured as a function of cavity length  $L$  at various temperatures. We determined the internal loss  $\alpha_0$  and internal differential quantum efficiency  $\eta_i$  from the slope and extrapolation according to the equation<sup>25-27</sup>

$$(\eta)^{-1} = (\eta_i)^{-1} \{1 + \alpha_0 L [\ln(1/R)]^{-1}\}, \quad (1)$$

where  $R = 0.32$  is the mirror reflectivity. As is well known, if the material is not uniform, the large scatter of the data generally causes large uncertainty in the values of  $\eta_i$  and  $\alpha_0$ . Careful selection of wafers to yield variation of less than 10% in both the threshold current and  $\eta$  is therefore necessary.

Figure 4 shows an example of the  $\phi$ - $I$  characteristics for a laser 610  $\mu\text{m}$  long. Near room temperature, the light output is linear to  $\sim 9$  mW from one cavity face. At lower temperatures, the curves become slightly super-linear at high power. The differential quantum efficiency in this case was determined from the straight-line portion of the curve just above the threshold, since we are only interested in the behavior near the threshold.

An example of the dependence of  $\eta^{-1}$  on the laser length  $L$  at 293 °K is shown in Fig. 5. All the data points follow quite well along a straight line. The values of  $\alpha_0$  and  $\eta_i$  are determined from the straight line which gives a least-squares fit to the data points.

Figures 6 and 7 show the obtained  $\eta_i$  and  $\alpha_0$  as a function of temperature. The vertical bars denote the standard deviation. The internal differential quantum efficiency is about 90% and is temperature independent. This means that almost every minority carrier that is injected across the junction is converted into a photon above the threshold. Although the waveguide in the direction parallel to the junction is defined by the current confinement, the near-unity  $\eta_i$  shows that the

fraction of carriers wasted to the low-gain region by carrier diffusion and current spreading is small near the threshold.

The temperature dependence of internal loss shown in Fig. 7 represents the first set of data ever reported for the stripe-geometry lasers. In most of the theoretical calculations<sup>3,10,13,14</sup> for the temperature dependence of the threshold current, it was generally assumed that the  $\alpha_0$  is independent of temperature. This naturally results in the saturation of the threshold current at lower temperatures. Our data here show that  $\alpha_0$  is a sensitive function of temperature, decreasing from  $\sim 34$   $\text{cm}^{-1}$  at 293 °K to nearly 2  $\text{cm}^{-1}$  at 10 °K. For a broad-contact laser, the internal loss consists of contributions from free-carrier absorption and scattering loss due to imperfect waveguide walls with the former dominating.<sup>28</sup> For a stripe-geometry laser, additional contribution from diffraction loss to the unpumped region outside of the stripe must be considered. The room-temperature internal loss is  $\sim 10$   $\text{cm}^{-1}$ <sup>23,29</sup> for a broad-contact laser with a carrier density of  $\sim 7 \times 10^{17}$   $\text{cm}^{-3}$ . Since it requires about a  $2 \times 10^{18}$   $\text{cm}^{-3}$  carrier concentration to reach the threshold for a strip-geometry laser with a 13- $\mu\text{m}$ -wide contact,<sup>19</sup> the free-carrier absorption loss should be  $\sim 28$   $\text{cm}^{-1}$ . This leaves 6  $\text{cm}^{-1}$  for the diffraction loss at room temperature. At low temperatures, the free-carrier absorption is negligible because of the lower carrier density required to reach the threshold. The value of 2  $\text{cm}^{-1}$  at 10 °K should be mainly caused by the diffraction. This is smaller than the corresponding value at room temperature, indicating a slight temperature-dependent diffraction loss.

### C. Theoretical calculation of the temperature dependence of threshold current

Many models have been used for the theoretical calculation of threshold current.<sup>3-14</sup> Depending on the re-

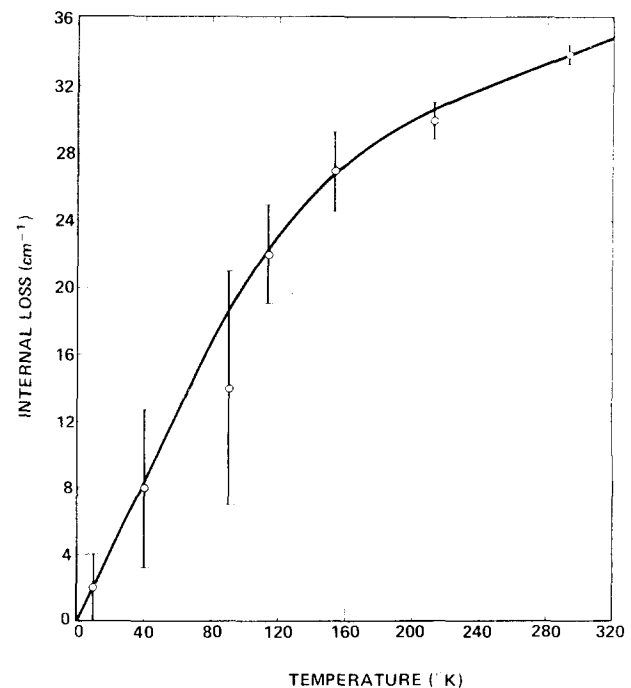


FIG. 7. Variation of the internal loss with temperature.

combination mechanisms, there are band-to-band,<sup>9,14</sup> band-to-impurity-states,<sup>30</sup> band-to-bandtail,<sup>31</sup> and bandtail-to-bandtail calculations.<sup>10-13</sup> The calculation on the band-to-band transition also depends on whether the recombination follows the  $\mathbf{k}$  selection rule. In all cases, however, the calculation involves computation of the gain as a function of current. The threshold current is taken as one which yields a gain equal to the cavity loss. Since the impurity concentration in the active layer is low ( $4 \times 10^{17} \text{ cm}^{-3}$ ) and is not compensated, the formation of appreciable bandtails in both bands is not likely. Calculation using perturbation techniques<sup>3</sup> shows that the distortion of the band shape by the presence of the impurities of such concentration is also negligible. We therefore think that the transition is likely to follow  $\mathbf{k}$  selection band to band at least for high temperatures ( $\geq 80^\circ\text{K}$ ), where most of the carriers occupy the high-energy states of the bands. Stern has done such a calculation for an active region which contains no impurities.<sup>14</sup> His calculation is obviously valid also for the cases when the injected carrier density is higher than the doped-impurity concentration. For example, the carrier densities required to reach the threshold for a laser with a cavity loss of  $50 \text{ cm}^{-1}$  are  $2.7 \times 10^{17} \text{ cm}^{-3}$  at  $80^\circ\text{K}$ ,  $7.2 \times 10^{17} \text{ cm}^{-3}$  at  $160^\circ\text{K}$ ,  $1.4 \times 10^{18} \text{ cm}^{-3}$  at  $250^\circ\text{K}$ , and  $1.8 \times 10^{18} \text{ cm}^{-3}$  at  $300^\circ\text{K}$ .<sup>14</sup> Thus, the calculation should be applicable in our case above  $\sim 80^\circ\text{K}$ .

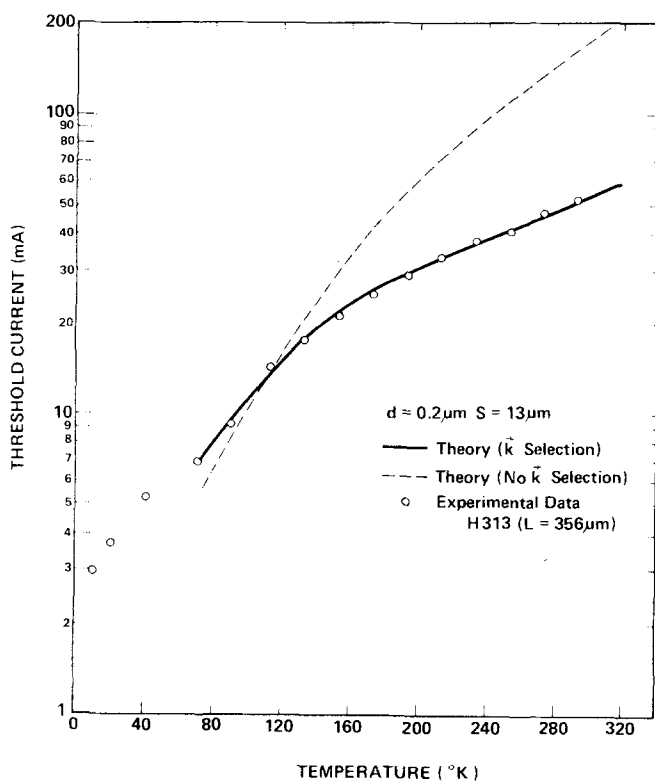


FIG. 8. Theoretical temperature dependence of the threshold current based on the band-to-band recombination with and without  $\mathbf{k}$  selection. The calculation is based on the theories of Stern's ( $\mathbf{k}$  selection), and Lasher and Stern's (no  $\mathbf{k}$  selection) using the temperature dependence of internal loss shown in Fig. 7. The vertical scale of the dashed curve is reduced by a factor of 3.3 for easy comparison. Experimental data on a laser  $356 \mu\text{m}$  long,  $13 \mu\text{m}$  wide, and  $0.2 \mu\text{m}$  thick are also shown for comparison.

Using the calculation of Stern,<sup>14</sup> the temperature dependence of the cavity loss, an active-layer thickness of  $0.2 \mu\text{m}$ , a laser length of  $356 \mu\text{m}$ , and a stripe width of  $13 \mu\text{m}$ , we obtain the solid curve shown in Fig. 8. The experimental points are also shown for comparison. The agreement is remarkable considering that there are no adjustable parameters in the calculation. However, the agreement may be fortuitous in the sense that the calculation contains so many parameters and involves so complicated a numerical computation that such perfect agreement is not expected. In any case, both the theory and the experiment give the same temperature variation of the threshold current. This is sufficient to show that at least above  $80^\circ\text{K}$ , the recombination is from the conduction band to the valence band and follows the  $\mathbf{k}$  selection rule. A band-to-band recombination mechanism was also deduced previously from the measurements of threshold current and lasing delay time in DH lasers.<sup>19</sup>

The change in threshold behavior from a relatively slow variation at high temperatures to a more rapid one below  $140^\circ\text{K}$  is not caused by a change in the recombination mechanism. It is a result of the combination of a more rapid decrease both in  $\alpha$  and in the current required to reach a given gain below  $140^\circ\text{K}$ , with the latter dominating. It is worth elaborating at least qualitatively at this point the significance of the slow increase in threshold current at higher temperatures since this makes cw operation possible at temperatures as high as  $112^\circ\text{C}$ .<sup>33</sup> At high temperatures, the carrier population spreads in a wider energy range. More carriers are thus required to reach a given gain, since only a small fraction of the population which recombines with a photon energy less than or equal to the difference between the electron and hole Fermi energies can contribute to gain<sup>9</sup>; the rest of the carriers are wasted in spontaneous recombination. In good carrier confinement devices such as DH lasers, the injection current is proportional to the total spontaneous recombination rate. There is little difference in the recombination rates with and without  $\mathbf{k}$  selection for those carriers which can contribute to the gain because they occupy only a narrow energy range near the band edges.<sup>34</sup> As far as achieving the same gain is concerned, about the same density of carriers is required regardless of whether the  $\mathbf{k}$  selection is followed or not. However, this same carrier density yields a much smaller total spontaneous recombination rate with selection rule since the recombination is restricted to carriers with the same  $\mathbf{k}$ .<sup>34</sup> The higher the temperature, the smaller the fraction of these carriers. We therefore expected that the current required to reach a given gain increases much slower with temperature if the transitions follow the  $\mathbf{k}$  selection. As a comparison, we plot in Fig. 8 (dashed curve) the calculated temperature dependence of threshold current in the case of nonselection rule transitions<sup>9</sup> using the same  $\alpha$  as for the  $\mathbf{k}$  selection case. The vertical scale of the curve is reduced by a factor of 3.3 for easy comparison. The current is seen to increase more rapidly at high temperatures. We therefore conclude that the change of temperature dependence of the threshold from a faster rate at low-

temperatures to a slower rate at high temperatures is a consequence of  $\mathbf{k}$  selection rule transitions.

#### IV. CONCLUSION

The temperature dependence of the threshold current has been measured for a wide range of impurity concentrations in the active region. At high temperatures ( $\geq 100^\circ\text{K}$ ), the threshold increases relatively slowly and the behavior is independent of the type and concentration of the impurity. Theoretical calculation using the measured cavity loss shows that this high-temperature behavior is to be expected for a band-to-band recombination which follows  $\mathbf{k}$  selection. The threshold current at low temperatures ( $\leq 80^\circ\text{K}$ ) decreases more rapidly with temperature but sometimes shows saturation depending on the type and concentration of the impurity. The higher the impurity concentration, the higher the saturation temperature. The saturation temperature is also higher for  $n$ -type active regions than for  $p$ -type active regions for the same impurity concentrations. The saturation is attributed to the carrier diffusion length becoming smaller than the active-layer thickness. While the internal differential quantum efficiency is independent of temperature, the internal loss decreases with temperature. The decrease in internal loss is caused mainly by the reduction in free-carrier absorption.

#### ACKNOWLEDGMENTS

We would like to thank R. J. Archer and P. E. Greene for valuable comments, and M. Burton, R. Drabin, T. Inouye, and B. Nolan for technical assistance in laser fabrication and testing.

<sup>1</sup>M. Pilkuhn, H. Rupprecht, and B. Blum, *Solid-State Electron.* **7**, 905 (1964).

<sup>2</sup>G. C. Dousmanis, H. Nelson, and D. L. Staebler, *Appl. Phys. Lett.* **5**, 174 (1964).

<sup>3</sup>J. I. Pankove, *IEEE J. Quantum Electron.* **QE-4**, 119 (1968).

<sup>4</sup>H. Kressel, H. F. Lockwood, and H. Nelson, *IEEE J. Quantum Electron.* **QE-6**, 278 (1970).

<sup>5</sup>I. Hayashi and M. Panish, *J. Appl. Phys.* **41**, 150 (1970).

<sup>6</sup>See, for example, J. E. Ripper and J. A. Rossi, *IEEE J. Quantum Electron.* **QE-10**, 435 (1974).

<sup>7</sup>J. E. Ripper and T. L. Paoli, *Proc. IEEE* **58**, 178 (1970).

<sup>8</sup>J. E. Ripper, T. L. Paoli, and J. C. Dymont, *IEEE J. Quantum Electron.* **QE-6**, 300 (1970).

<sup>9</sup>G. Lasher and F. Stern, *Phys. Rev.* **133**, A553 (1964).

<sup>10</sup>F. Stern, *Phys. Rev.* **148**, 186 (1966).

<sup>11</sup>C. J. Hwang, *Phys. Rev. B* **2**, 4117 (1970).

<sup>12</sup>C. J. Hwang, *Phys. Rev. B* **2**, 4126 (1970).

<sup>13</sup>F. Stern, in *Laser Handbook* (Norht-Holland, Amsterdam, 1972).

<sup>14</sup>F. Stern, *IEEE J. Quantum Electron.* **QE-9**, 290 (1973).

<sup>15</sup>I. Hayashi, M. P. Panish, and F. K. Reinhart, *J. Appl. Phys.* **42**, 1929 (1971).

<sup>16</sup>H. Kressel, in *Lasers*, edited by A. K. Levine and A. J. DeMaria (Marcel Dekker, New York, 1971), Vol. 3, p. 2.

<sup>17</sup>R. L. Hartman, J. C. Dymont, C. J. Hwang, and M. Kuhn, *Appl. Phys. Lett.* **23**, 181 (1973).

<sup>18</sup>J. C. Dymont, L. A. D'Asaro, J. C. North, B. I. Miller, and J. E. Ripper, *Proc. IEEE* **60**, 726 (1972).

<sup>19</sup>C. J. Hwang and J. C. Dymont, *J. Appl. Phys.* **44**, 3240 (1973).

<sup>20</sup>R. Kubo, *J. Phys. Soc. Jpn.* **12**, 570 (1957); E. Spenke, *Electronic Semiconductors* (McGraw-Hill, New York, 1958), p. 295.

<sup>21</sup>C. J. Hwang, *J. Appl. Phys.* **42**, 757 (1971).

<sup>22</sup>E. J. Moore, *Phys. Rev.* **160**, 618 (1967).

<sup>23</sup>H. Brooks, *Phys. Rev.* **83**, 879 (1951).

<sup>24</sup>R. B. Dingle, *Philos. Mag.* **46**, 831 (1955).

<sup>25</sup>J. R. Biard, W. N. Carr, and B. S. Reed, *Trans. Metall. Soc. AIME* **230**, 286 (1964).

<sup>26</sup>V. P. Gribkovskii, V. K. Kononenko, and V. A. Samoilynovich, *Phys. Status Solidi A* **3**, 353 (1970).

<sup>27</sup>M. H. Pilkuhn, *Phys. Status Solidi* **25**, 9 (1968).

<sup>28</sup>E. Pinkas, B. I. Miller, I. Hayashi, and P. W. Foy, *IEEE J. Quantum Electron.* **QE-9**, 281 (1973).

<sup>29</sup>Zh. I. Alferov, V. M. Andreev, E. L. Portnoi, and M. K. Trukan, *Sov. Phys.-Semicond.* **3**, 1107 (1970).

<sup>30</sup>W. P. Dumke, *Phys. Rev.* **132**, 1998 (1963).

<sup>31</sup>G. J. Burrell, T. S. Moss, and A. Hetherington, *Solid-State Electron.* **12**, 787 (1969).

<sup>32</sup>See, for example, V. L. Bonch-Bruевич, in *Semiconductors and Semimetals*, edited by R. K. Willardson and A. C. Beer (Academic, New York, 1966), Vol. 1, p. 101.

<sup>33</sup>R. L. Hartman and R. W. Dixon, *Appl. Phys. Lett.* **26**, 239 (1975).

<sup>34</sup>See, for example, the comparison of the calculated results by M. J. Adams and P. T. Landsberg, in *Gallium Arsenide Lasers*, edited by C. H. Gooch (Wiley-Interscience, London, 1969), p. 6.